

Active control of delaminated composite shells with piezoelectric sensor/actuator patches

Namita Nanda* and Y. Nath^a

Department of Applied Mechanics, Indian Institute of Technology Delhi, New Delhi, 110016, India

(Received November 30, 2010, Revised February 9, 2012, Accepted March 18, 2012)

Abstract. Present study deals with the development of finite element based solution methodology to investigate active control of dynamic response of delaminated composite shells with piezoelectric sensors and actuators. The formulation is based on first order shear deformation theory and an eight-noded isoparametric element is used. A coupled piezoelectric-mechanical formulation is used in the development of the constitutive equations. For modeling the delamination, multipoint constraint algorithm is incorporated in the finite element code. A simple negative feedback control algorithm coupling the direct and converse piezoelectric effects is used to actively control the dynamic response of delaminated composite shells in a closed loop employing Newmark's time integration scheme. The validity of the numerical model is demonstrated by comparing the present results with those available in the literature. A number of parametric studies such as the locations of sensor/actuator patches, delamination size and its location, radius of curvature to width ratio, shell types and loading conditions are carried out to understand their effect on the transient response of piezoceramic delaminated composite shells.

Keywords: active control; delamination; composite; shell; finite element; smart material

1. Introduction

Active sensing and control of dynamic systems using piezoelectric materials have been the subject of significant amount of research in recent years. These materials induce an electric potential/charge when they are subjected to a mechanical load, which is called the direct piezoelectric effect. Conversely, mechanical deformation or strain is produced due to the externally applied electric potential, which is called the converse piezoelectric effect. Use of piezoelectric materials as distributed sensors and actuators in the active control of dynamic systems is attributed to these two phenomena. Vibration control of laminated plates with piezoelectric sensors/actuators have been extensively studied using FE models (Tzou and Tseng 1990, Chandrashekhara and Agarwal 1993, Hwang and Park 1993, Samanta *et al.* 1996, Lam *et al.* 1997, Wang *et al.* 2001, Moita *et al.* 2004). Vibration control of composites containing piezoelectric polymers has been studied by Lammering (1991) using finite shell element. Balamurugan and Narayanan (2001) presented shell finite element for active vibration control of smart piezoelectric composite plate/shell structures. They used a C^0

*Corresponding author, Research Associate, E-mail: namita_nanda@rediffmail.com

^aProfessor, E-mail: ynath@am.iitd.ac.in

continuous, shear flexible, nine noded quadrilateral shell element based on field consistency principle. Ray and Reddy (2005) dealt with the analysis of active constrained layer damping of laminated thin composite shells using piezoelectric fiber reinforced composite materials. Vel and Baillargeon (2005) presented an analytical solution for the static deformation and steady-state vibration of composite cylindrical shells with embedded piezoelectric sensors and actuators. The static and dynamic responses of laminated composite shells containing integrated piezoelectric sensors and actuators subjected to electrical, mechanical and thermal loadings were modeled by Kumar *et al.* (2008) using FE formulation. The formulation was based on the first order shear deformation theory and Hamilton's principle.

While designing with smart composites, it is important to take into consideration imperfections, such as delaminations, that are often pre-existing or are post-generated during service life. Delamination, which is a debonding or separation between individual plies, will have significant impact on performance of piezoelectric actuator and vibration characteristics of the aerospace, mechanical, civil and offshore structures due to degradation of overall stiffness and strength. A significant amount of research has been carried out on the vibration analysis of delaminated composite beams and plates (Shen and Grady 1992, Ju *et al.* 1995, Kim *et al.* 2003, Zhu *et al.* 2005, Oh *et al.* 2005, Aymerich *et al.* 2009, Park *et al.* 2009). However, a limited research has been conducted on investigating the effects of delamination on the dynamic response of composite shells. The free vibration and transient responses of multiple delaminated cylindrical and spherical panels subjected to hygrothermal environments were analyzed by Parhi *et al.* (2001) using the first order shear deformation theory. Kim and Cho (2003) presented an efficient higher order shell theory for laminated composites with multiple delaminations. The dynamic stability analysis of delaminated spherical shell structures subjected to in-plane pulsating forces was carried out by Park and Lee (2009) using the higher order shell theory. A few studies on the dynamic response analysis of adaptive composite plates with surface bonded/embedded piezoelectric actuators and sensors including delamination are due to Chattopadhyay *et al.* (2004), Ghosal *et al.* (2005) and Kim *et al.* (2006).

The review of literature shows that dynamic response of delaminated composite shells with piezoelectric sensors and actuators is yet to receive its due attention in spite of the well known existence of delaminations in the practical applications of such shells. Hence in this article, a study on active control of dynamic response of delaminated composite shells with piezoelectric sensors and actuators is carried out using the finite element method developed here. To ensure compatibility of deformation and equilibrium of forces and moments at the delamination surface, multipoint constraint algorithm is incorporated in the finite element code. The effect of different practical parametric variations such as the locations of sensor/actuator patches, delamination size and its location, radius of curvature to width ratio, shell types and loading conditions on the dynamic response of piezoceramic delaminated composite shells are studied to arrive at interference of engineering significance.

2. Theory and formulation

2.1 Constitutive equations

The constitutive relations of a piezoelectric layer (Tiersten 1969) can be written as

$$\{\hat{\sigma}\} = [Q]\{\hat{\varepsilon}\} - [e]^T\{E\} \tag{1}$$

$$\{H\} = [e]\{\hat{\varepsilon}\} + [p]\{E\} \tag{2}$$

where $\{\hat{\sigma}\}$ is the stress, $\{\hat{\varepsilon}\}$ is the strain, $[Q]$ is the elastic stiffness matrix, $[e]$ is the piezoelectric stress coefficient matrix, $\{E\}$ is the electric field intensity, $\{H\}$ is the electric displacement and $[p]$ is the permittivity matrix.

The piezoelectric stress coefficient matrix $[e]$ can be expressed in terms of the more commonly available piezoelectric strain coefficient matrix $[d]$ as

$$[e] = [d][Q] \tag{3}$$

Substituting Eq. (3) into Eq. (1)

$$\{\hat{\sigma}\} = [Q](\{\hat{\varepsilon}\} - [d]^T\{E\}) \tag{4}$$

The piezoelectric strain can be written as

$$\{\hat{\varepsilon}\}_p = \begin{bmatrix} 0 & 0 & d_{31} \\ 0 & 0 & d_{32} \\ 0 & 0 & d_{33} \\ 0 & d_{24} & 0 \\ d_{15} & 0 & 0 \end{bmatrix} \begin{Bmatrix} 0 \\ 0 \\ E \end{Bmatrix} \tag{5}$$

or

$$\{\hat{\varepsilon}\}_p = E\{d\} \tag{6}$$

where

$$\{d\} = (d_{31} \ d_{32} \ d_{33} \ 0 \ 0)^T \tag{7}$$

Hence, for k th layer Eq. (1) can be written as

$$\{\hat{\sigma}\}_k = [Q]_k\{\hat{\varepsilon}\}_k - E_k[Q]_k\{d\} \tag{8}$$

Eq. (8) is with reference to the principal material axes of the lamina. It is necessary to transform the constitutive relation for any arbitrary axis. Thus, for k th layer

$$\{\sigma\}_k = [\bar{Q}]_k\{\varepsilon'\}_k - E_k[\bar{Q}]_k\{d\} \tag{9}$$

The transformation relations for various quantities in the lamina and shell coordinate systems can be found in the textbook by Reddy (2004).

2.2 Strain-displacement relations

The displacement field based on first order shear deformation theory is given by

$$U(x, y, z) = u(x, y) + z\theta_x(x, y) \quad (10a)$$

$$V(x, y, z) = v(x, y) + z\theta_y(x, y) \quad (10b)$$

$$W(x, y, z) = w(x, y) \quad (10c)$$

where, U , V and W are the displacements at any point (x, y, z) of the shell in x, y and z directions, respectively; u , v and w are the associated mid-plane displacements; and θ_x and θ_y are the rotations about y and x axes, respectively. The strain-displacement relations are given by

$$\varepsilon'_x = \varepsilon_x + z\kappa_x \quad (11a)$$

$$\varepsilon'_y = \varepsilon_y + z\kappa_y \quad (11b)$$

$$\gamma'_{xy} = \gamma_{xy} + z\kappa_{xy} \quad (11c)$$

$$\gamma'_{xz} = \gamma_{xz} \quad (11d)$$

$$\gamma'_{yz} = \gamma_{yz} \quad (11e)$$

where $\varepsilon_x, \varepsilon_y, \gamma_{xy}$ are the in-plane strains, γ_{xz}, γ_{yz} are the shear strains and $\kappa_x, \kappa_y, \kappa_{xy}$ are the curvatures.

Above equations can be written as

$$\{\varepsilon'\} = \{\varepsilon\} + z\{\kappa\} \quad (12)$$

where

$$\{\varepsilon'\} = (\varepsilon'_x \ \varepsilon'_y \ \gamma'_{xy} \ \gamma'_{xz} \ \gamma'_{yz})^T \quad (13a)$$

$$\{\varepsilon\} = (\varepsilon_x \ \varepsilon_y \ \gamma_{xy} \ \gamma_{xz} \ \gamma_{yz})^T \quad (13b)$$

$$\{\kappa\} = (\kappa_x \ \kappa_y \ \kappa_{xy} \ 0 \ 0)^T \quad (13c)$$

The mid-surface kinematic relations of Sanders shell theory can be written as

$$\varepsilon_x = \partial u / \partial x + w / R_x \quad (14a)$$

$$\varepsilon_y = \partial v / \partial y + w / R_y \quad (14b)$$

$$\gamma_{xy} = \partial u / \partial y + \partial v / \partial x + 2w / R_{xy} \quad (14c)$$

$$\gamma_{xz} = \theta_x + \partial w / \partial x - u / R_x - v / R_{xy} \quad (14d)$$

$$\gamma_{yz} = \theta_y + \partial w / \partial y - v / R_y - u / R_{xy} \quad (14e)$$

$$\kappa_x = \partial \theta_x / \partial x \quad (14f)$$

$$\kappa_y = \partial \theta_y / \partial y \quad (14g)$$

$$\kappa_{xy} = \partial \theta_x / \partial y + \partial \theta_y / \partial x + C_0(\partial v / \partial x - \partial u / \partial y) \quad (14h)$$

where R_x and R_y are the radii of curvature of the shell along x and y directions, respectively, and R_{xy} is the twist radius of curvature. The term $C_0 = 0.5(1/R_y - 1/R_x)$ is the result of Sanders' theory (Sanders 1959) which accounts for the condition of zero strain for rigid body motion.

An eight-noded isoparametric element is used with five degrees of freedom viz. u , v , w , θ_x and θ_y at each node. The displacement vector at any point on the mid-plane $\{\delta\}$ is defined in terms of nodal displacement vector $\{\delta_e\}$ and shape function matrix $[N]$ as

$$\{\delta\} = [N]\{\delta_e\} \quad (15)$$

where,

$$\{\delta\} = \{u \ v \ w \ \theta_x \ \theta_y\}^T, \quad \{\delta_e\} = \{u_i \ v_i \ w_i \ \theta_{xi} \ \theta_{yi}\}^T \quad i = 1, 2, \dots, 8 \quad (16)$$

$$[N] = \begin{bmatrix} N_i & 0 & 0 & 0 & 0 \\ 0 & N_i & 0 & 0 & 0 \\ 0 & 0 & N_i & 0 & 0 \\ 0 & 0 & 0 & N_i & 0 \\ 0 & 0 & 0 & 0 & N_i \end{bmatrix} \quad i = 1, 2, \dots, 8 \quad (17)$$

The generalized strain vectors $\{\bar{\varepsilon}\}$ corresponding to the mid-plane can be written as

$$\{\bar{\varepsilon}\} = \{\varepsilon_x \ \varepsilon_y \ \gamma_{xy} \ \kappa_x \ \kappa_y \ \kappa_{xy} \ \gamma_{xz} \ \gamma_{yz}\}^T \quad (18)$$

From Eqs. (14) and (15), Eq. (18) can be written as

$$\{\bar{\varepsilon}\} = [B]\{\delta_e\} \quad (19)$$

where $[B]$ is the strain-displacement matrix.

$$[B] = \begin{bmatrix} \partial N_i / \partial x & 0 & N_i / R_x & 0 & 0 \\ 0 & \partial N_i / \partial y & N_i / R_y & 0 & 0 \\ \partial N_i / \partial y & \partial N_i / \partial x & 2N_i / R_{xy} & 0 & 0 \\ 0 & 0 & 0 & \partial N_i / \partial x & 0 \\ 0 & 0 & 0 & 0 & \partial N_i / \partial y \\ -C_0 \partial N_i / \partial y & C_0 \partial N_i / \partial x & 0 & \partial N_i / \partial y & \partial N_i / \partial x \\ -N_i / R_x & -N_i / R_{xy} & \partial N_i / \partial x & N_i & 0 \\ -N_i / R_{xy} & -N_i / R_y & \partial N_i / \partial y & 0 & N_i \end{bmatrix} \quad i = 1, 2, \dots, 8 \quad (20)$$

The constitutive relation can be written as

$$\{\bar{N}\} = [D]\{\bar{\varepsilon}\} - \{\bar{N}_p\} \quad (21)$$

where $\{\bar{N}\}$ is the stress and moment resultant vector defined by

$$\{\bar{N}\} = \{N_x \ N_y \ N_{xy} \ M_x \ M_y \ M_{xy} \ Q_x \ Q_y\}^T \quad (22)$$

$$(N_x \ N_y \ N_{xy} \ Q_x \ Q_y) = \sum_{k=1}^n \int_{z_{k-1}}^{z_k} (\sigma_x \ \sigma_y \ \tau_{xy} \ \tau_{xz} \ \tau_{yz}) dz \quad (23)$$

$$\{M_x \ M_y \ M_{xy}\} = \sum_{k=1}^n \int_{z_{k-1}}^{z_k} (\sigma_x \ \sigma_y \ \tau_{xy}) z dz \quad (24)$$

The constitutive stiffness matrix $[D]$ is given by

$$[D] = \begin{bmatrix} A_{11} & A_{12} & A_{16} & B_{11} & B_{12} & B_{16} & 0 & 0 \\ A_{12} & A_{22} & A_{26} & B_{12} & B_{22} & B_{26} & 0 & 0 \\ A_{16} & A_{26} & A_{66} & B_{16} & B_{26} & B_{66} & 0 & 0 \\ A_{11} & A_{12} & A_{16} & D_{11} & D_{12} & D_{16} & 0 & 0 \\ A_{12} & A_{22} & A_{26} & D_{12} & D_{22} & D_{26} & 0 & 0 \\ A_{16} & A_{26} & A_{66} & D_{16} & D_{26} & D_{66} & 0 & 0 \\ 0 & 0 & 0 & 0 & 0 & 0 & S_{44} & S_{45} \\ 0 & 0 & 0 & 0 & 0 & 0 & S_{45} & S_{55} \end{bmatrix} \quad (25)$$

The elements of the stiffness matrix $[D]$ are defined as

$$[A_{ij}, B_{ij}, D_{ij}] = \sum_{k=1}^n \int_{z_{k-1}}^{z_k} (\bar{Q}_{ij})_k (1, z, z^2) dz \quad (i, j = 1, 2, 6) \quad (26)$$

$$S_{ij} = \sum_{k=1}^n \kappa \int_{z_{k-1}}^{z_k} (\bar{Q}_{ij})_k dz \quad (i, j = 4, 5) \quad (27)$$

where κ , the shear correction factor, is assumed as $5/6$.

The stress and moment resultant vector $\{\bar{N}_p\}$ due to due to the piezoelectric actuator is given by

$$\{\bar{N}_p\} = [P]\{d\} \quad (28)$$

where

$$[P] = \begin{bmatrix} P_{11} & P_{12} & P_{16} & 0 & 0 \\ P_{12} & P_{22} & P_{26} & 0 & 0 \\ P_{16} & P_{26} & P_{66} & 0 & 0 \\ W_{11} & W_{12} & W_{16} & 0 & 0 \\ W_{12} & W_{22} & W_{26} & 0 & 0 \\ W_{16} & W_{26} & W_{66} & 0 & 0 \\ 0 & 0 & 0 & 0 & 0 \\ 0 & 0 & 0 & 0 & 0 \end{bmatrix} \quad (29)$$

$$P_{ij} = \sum_{k=1}^n \int_{z_{k-1}}^{z_k} E_k(\bar{Q}_{ij})_k dz = \sum_{k=1}^n V_k(\bar{Q}_{ij})_k \quad (i, j = 1, 2, 6) \quad (30)$$

$$W_{ij} = \sum_{k=1}^n \int_{z_{k-1}}^{z_k} E_k(\bar{Q}_{ij})_k z dz = \sum_{k=1}^n V_k(\bar{Q}_{ij})_k z_k^0 \quad (i, j = 1, 2, 6) \quad (31)$$

where

$$E_k = V_k/h_k \quad (32)$$

V_k is the electric voltage across the k th layer, h_k is the thickness of the k th layer and z_k^0 is the z distance of the lamina mid-plane defined by

$$z_k^0 = 1/2(z_k + z_{k-1}) \quad (33)$$

2.3 Delamination modeling

Fig. 1 shows a laminated composite shell with delamination. The undelaminated region is modeled by element 1 of thickness h and the delaminated region is modeled by elements 2 and 3 (Fig. 2) whose interface contains the considered delamination (Park *et al.* 2009). The displacements are represented by

$$U_l(x, y, x) = u_l(x, y) + (z - z_l)\theta_x(x, y) \quad (34a)$$

$$V_l(x, y, x) = v_l(x, y) + (z - z_l)\theta_y(x, y) \quad (34b)$$

$$W_l(x, y, x) = w_l(x, y) \quad (34c)$$

where, $z_l(l = 2, 3)$ is the z co-ordinate of mid-plane of element l .

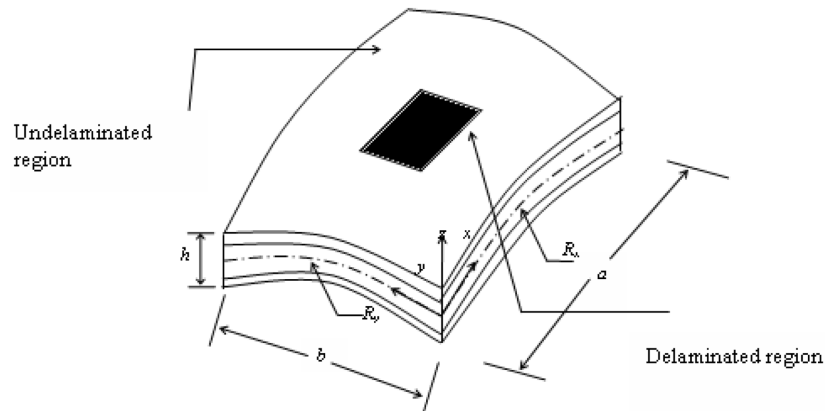


Fig. 1 Laminated composite shell with delamination

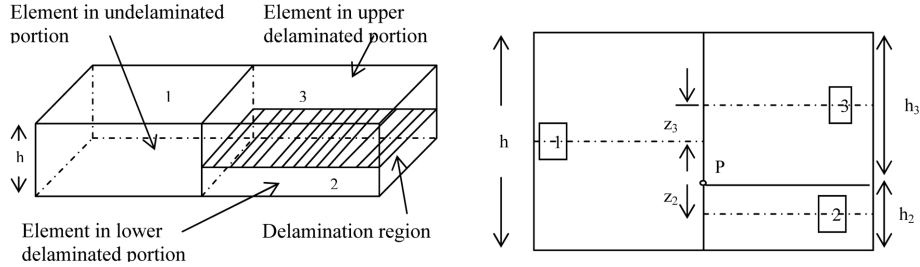


Fig. 2 Elements at connecting boundaries between undelaminated and delaminated portions

In order to ensure the continuity of displacements at the delaminated edge, it is assumed that transverse displacement (w) and rotations (θ_x, θ_y) at a common node are equal

$$w_1 = w_2 = w_3 = w \quad (35a)$$

$$\theta_{x1} = \theta_{x2} = \theta_{x3} = \theta_x \quad (35b)$$

$$\theta_{y1} = \theta_{y2} = \theta_{y3} = \theta_y \quad (35c)$$

The displacement-based multipoint constraints are introduced (Eq. (35a)-(35c)) into the kinematic relations to ensure the connectivity of the delaminated region with the undelaminated part of the laminate. The in-plane displacements of delaminated elements are

$$u_l(x, y) = u(x, y) + z_l \theta_x(x, y) \quad (35d)$$

$$v_l(x, y) = v(x, y) + z_l \theta_y(x, y) \quad (35e)$$

The strain components are derived as

$$\{\varepsilon'\}_l = \{\varepsilon\} + z_l \{\kappa\} \quad l = 2, 3 \quad (36)$$

Following the delamination model proposed by Gim (1994), the numerical procedures have been developed for modeling delamination in composite laminates. A displacement based multipoint constraints, i.e., Eqs. (35) and (36), are imposed on the kinematics to ensure the compatibility of deformation and the equilibrium of resultant forces and moments at the delaminated edge (Gim 1994). Accordingly, the stress and moment resultants are obtained as follows

$$\{\bar{N}\} = [D]_l \{\bar{\varepsilon}\}_l - \{\bar{N}_p\} \quad (37)$$

where,

$$[D]_l = \begin{bmatrix} A_{ij} & z_l A_{ij} + B_{ij} & 0 \\ B_{ij} & z_l A_{ij} + D_{ij} & 0 \\ 0 & 0 & S_{ij} \end{bmatrix} \quad (38)$$

$$[A_{ij}, B_{ij}, D_{ij}]_l = \sum_{k=1}^n \int_{-h_l/2+z_i}^{h_l/2+z_i} (\bar{Q}_{ij})_k [1, (z-z_l), (z-z_l)^2] dz \quad (i, j = 1, 2, 6) \quad (39)$$

$$[S_{ij}]_l = \sum_{k=1}^n \kappa \int_{-h_l/2+z_i}^{h_l/2+z_i} (\bar{Q}_{ij})_k dz \quad (i, j = 4, 5) \quad (40)$$

Thus, the delamination reduces the mechanical stiffness of the lamina.

2.4 Governing equations of motion

The governing equation of motion (Chandrashekhara and Agarwal 1993) is given by

$$[M_e]\{\ddot{\delta}_e\} + [C_e]\{\dot{\delta}_e\} + ([K_e])\{\delta_e\} = \{R_e\} + \{R_e^p\} \quad (41)$$

where $\{\delta_e\}$, $\{\dot{\delta}_e\}$ and $\{\ddot{\delta}_e\}$ are the generalized displacement, velocity and acceleration vectors, respectively; $[M_e]$, $[C_e]$ and $[K_e]$ are the mass, damping and stiffness matrices, respectively; $\{R_e\}$ is the external force vector; and $\{R_e^p\}$ is the actuator force vector.

$$[M_e] = \int_A [N]^T [\rho] [N] dA \quad (42a)$$

$$[K_e] = \int_A [B]^T [D] [B] dA \quad (42b)$$

$$\{R_e\} = \int_A [N]^T [q] dA \quad (42c)$$

$$\{R_e^p\} = \int_A [B]^T \{\bar{N}_p\} dA = [K_e^{av}] V \quad (42d)$$

where $[K_e^{av}]$ is the electromechanical coupling matrix of the piezoelectric actuators and $\{V\}$ is the actuator voltage vector.

Assembling the element equations, the global dynamic equation can be written as

$$[M]\{\ddot{\delta}\} + [C]\{\dot{\delta}\} + ([K])\{\delta\} = \{R\} + [K_{av}]\{V\} \quad (43)$$

2.5 Sensor equation

Substituting Eq. (3) into Eq. (2), for k th layer

$$\{H\}_k = [d][Q]_k \{\hat{\varepsilon}\}_k + [p]\{E\}_k \quad (44)$$

Since no external electric field is applied to the sensor layer that is poled in the z -direction, only the electric displacement H_3 is of interest. Using Eq. (7), we get

$$(H_3)_k = \{d\}^T [Q]_k \{\hat{\varepsilon}\}_k \quad (45)$$

Performing standard transformation, the above equation can be expressed as

$$(\bar{H}_3)_k = \{d\}^T [\bar{Q}]_k \{\varepsilon'\}_k \quad (46)$$

Using Eq. (12) in Eq. (46), gives

$$(\bar{H}_3)_k = \{d\}^T [\bar{Q}]_k (\{\varepsilon\} + z\{\kappa\}) \quad (47)$$

Now, the charge output of the sensor can be expressed in terms of spatial integration of $(\bar{H}_3)_k$ over its surface as

$$Q^{(S)}_t = \int_A (\bar{H}_3)_k dA = \frac{1}{2} \left[\int_A (\bar{H}_3)_k dA \Big|_{z=z_k} + \int_A (\bar{H}_3)_k dA \Big|_{z=z_{k-1}} \right] \quad (48)$$

Substituting Eq. (47) in Eq. (48) and using Eq. (33) results in

$$Q^{(S)}(t) = \int_A \{d\}^T [\bar{Q}]_k (\{\varepsilon\} + z\{\kappa\}) dA \quad (49)$$

which can be written as

$$Q^{(S)} = \int_A \{d\}^T [\bar{Q}]_k [H^S] \{\delta\} dA = [K_{sv}] \{\delta\} \quad (50)$$

where $[K_{sv}]$ is the electromechanical coupling matrix of the piezoelectric sensors. $[H^S]$ is defined by

$$[H^S] = \begin{bmatrix} \partial N_i / \partial x & 0 & N_i / R_x & z_k^0 (\partial N_i / \partial x) & 0 \\ 0 & \partial N_i / \partial y & N_i / R_y & 0 & z_k^0 (\partial N_i / \partial y) \\ (1 - z_k^0 C_0) \partial N_i / \partial y & (1 + z_k^0 C_0) \partial N_i / \partial x & 2N_i / R_{xy} & z_k^0 (\partial N_i / \partial y) & z_k^0 (\partial N_i / \partial x) \\ -N_i / R_x & -N_i / R_{xy} & \partial N_i / \partial x & N_i & 0 \\ -N_i / R_{xy} & -N_i / R_y & \partial N_i / \partial y & 0 & N_i \end{bmatrix} \quad (51)$$

The current on the surface of sensor is given by

$$I(t) = dQ^{(S)} / dt \quad (52)$$

When the piezoelectric sensor is used as strain rate sensor, the current can be converted into the open circuit sensor voltage output V^S as

$$V^S(t) = G_c I(t) = G_c (dQ^{(S)} / dt) \quad (53)$$

where G_c is the gain of the current amplifier, which transforms the sensor current to voltage.

2.6 Active control of damping

The sensor output voltage can be fed back through an amplifier to the actuator using a control algorithm. The actuating voltage V^e under a constant gain control algorithm can be expressed as

$$V^e = G_i V^s = G_i G_c (dQ^{(s)}/dt) \quad (54)$$

where G_i is the gain of the amplifier to provide feedback control.

Substituting Eq. (50) into Eq. (54), the system actuating voltage can be written as

$$V = G[K_{sv}]\{\dot{\delta}\} \quad (55)$$

where G is the control gain matrix given by

$$G = G_i G_c \quad (56)$$

Using Eq. (55) into Eq. (43) introduces an equivalent negative velocity feedback, and the equation of motion becomes

$$[M]\{\ddot{\delta}\} + ([C] + [C_A])\{\dot{\delta}\} + ([K])\{\delta\} = \{R\} \quad (57)$$

where $[C_A]$ is the active damping matrix given by

$$[C_A] = -[K_{av}]G[K_{sv}] \quad (58)$$

As shown in Eq. (57), the voltage control algorithm (Eq. (54)) has a damping effect on the vibration suppression of a distributed system. The solution of Eq. (57) is carried out using Newmark direct method of time integration (Reddy 2004 and Bathe 2001).

3. Results and discussion

A number of examples are solved to study the active control of dynamic response of delaminated composite shells with piezoelectric sensors and actuators using the finite element method. In all the numerical computations, the selective integration rule is employed. A 3×3 Gaussian rule is used to compute the in-plane, coupling between in-plane and bending and bending deformations, while a 2×2 rule is used to evaluate the terms associated with the transverse shear deformation. The simply supported boundary condition (Fig. 1) used in the present study is represented by

$$v = w = \theta_y = 0 \text{ at } x = 0, x = a \text{ and } u = w = \theta_x = 0 \text{ at } y = 0, y = b$$

Based on convergence study, the mesh size of 8×8 has been used throughout the study.

Cantilever and simply supported plate problems are considered to validate the program of the finite element formulation developed here. First, a cantilever laminated composite plate ($a = b = 200$ mm) bonded with piezoelectric actuators on upper and lower surfaces is considered to study the actuator's effect on the shape control. The stacking sequence of the composite plate is

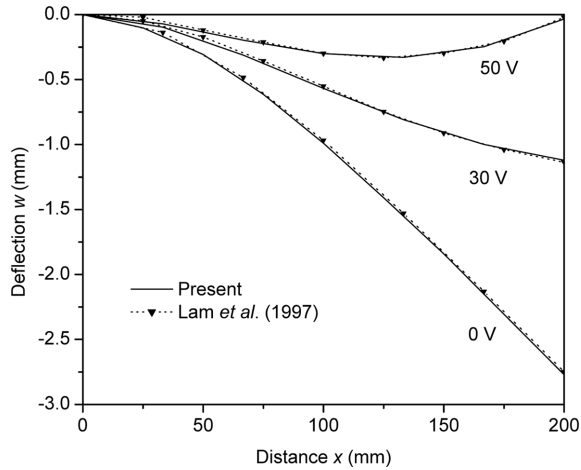


Fig. 3 Variation of centerline deflection of cantilever plate under uniformly distributed load with different actuator input voltage

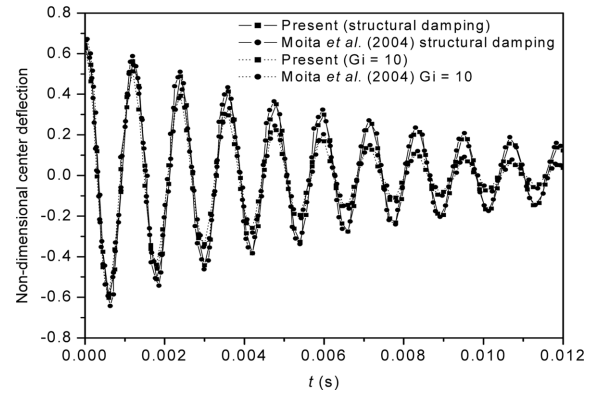


Fig. 4 Effect of structural damping and active control on the center deflection response of simply supported square laminated plate

–45/45/–45/45. The substrate is made of T300/976 graphite-epoxy composite and the piezoelectric layers are made of PZT G1195N and their corresponding material properties can be found in Lam *et al.* (1997). The plate is subjected to an uniformly distributed load of 100 N/m^2 . Fig. 3 shows the authors' results of centerline deflection of the composite plate under different active input voltages along with those of Lam *et al.* (1997). It can be seen that the results are in good agreement.

Next, a simply supported square laminated plate with lamination sequence 0/90/0, bonded with piezoelectric actuator and sensor layers on upper and lower surfaces is considered. The dimension of the plate is $a = b = 180 \text{ mm}$ and the thickness of the substrate layers and piezo-layer are 2 mm and 0.1 mm , respectively. The material properties are given in Moita *et al.* (2004). Rayleigh type damping is considered with coefficients $\alpha = 1 \times 10^{-6}$ and $\beta = 0.965 \times 10^{-5}$. The value of charge amplifier gain G_c is taken as $1.6 \times 10^7 \Omega$. The plate is subjected to a suddenly applied uniformly distributed load $q = 1000 \text{ N/m}^2$.

The non-dimensional center deflection is given by $\hat{w} = 100(E_{22}h^3/a^4q)w$, where E_{22} is the transverse moduli of the substrate layers and h is the total thickness of the plate. Fig. 4 presents the authors' results of both the structural damping and controlled ($G_i = 10$) non-dimensional center deflection response of the plate along with those of Moita *et al.* (2004). The comparison shows good agreement between the two sets of results.

Having validated the code, a number of parametric studies are carried out to understand the control of transient response of delaminated composite shells with piezoceramic PZT G1195N sensor/actuator patches. The material properties (Lam *et al.* 1997) of the substrate layer are: $E_{11} = 144.23 \text{ GPa}$, $E_{22} = 9.65 \text{ GPa}$, $G_{23} = 3.45 \text{ GPa}$, $G_{12} = G_{13} = 4.14 \text{ GPa}$, $\nu_{12} = 0.3$, $\rho = 1389.23 \text{ kg/m}^3$. For PZT G1195N, the following properties are used: $E_p = 63 \text{ GPa}$, $G_p = 24.2 \text{ GPa}$, $\nu_p = 0.28$, $\rho = 7600 \text{ kg/m}^3$. The shell dimensions considered are: $a = b = 0.254 \text{ m}$, $h = 2.54 \times 10^{-3} \text{ m}$ and the thickness of the piezoceramic patch is taken as $h = 2.0 \times 10^{-4} \text{ m}$. The locations of the delaminations A, B and C are determined by L_x/a and L_y/b whose co-ordinates $(L_x/a, L_y/b)$ are $(0, 0)$, $(0, 0.25)$ and $(0.25, 0.25)$, respectively, as indicated in Fig. 5. Four pairs of piezoceramic sensors and actuators are bonded on both the top and bottom surfaces of the composite shell in various locations

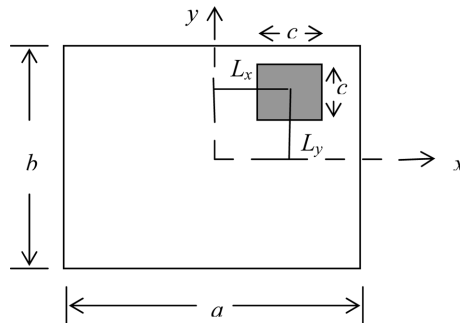
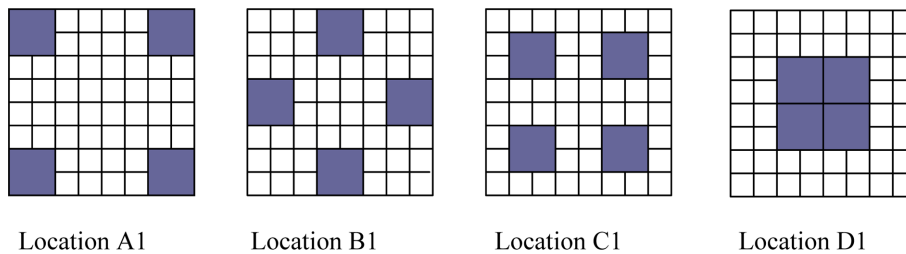
Fig. 5 Delamination location $(L_x/a, L_y/b)$ in the mid-plane

Fig. 6 Schematic diagram showing four locations of piezoelectric patches

A1-D1 as depicted in Fig. 6. Unless otherwise mentioned, a simply supported eight layer symmetric cross ply (0/90/0/90/90/0/90/0) delaminated spherical shell ($R_x = R_y = R$) in patch location A1 with gain value of 200 is considered in the analysis. The shells are subjected to a uniform step load of $q = 1000 \text{ N/m}^2$ and a time step of $\Delta t = 1 \text{ ms}$ is used for the Newmark method. Rayleigh type damping is considered with coefficients $\alpha = 1 \times 10^{-6}$ and $\beta = 0.965 \times 10^{-5}$. A single square mid-plane delamination of size $c/a = 0.5$, where c is the span of delamination, located at the center (type A) of the shell ($R/b = 10$) is considered.

3.1 Active vibration control for the transient response

Fig. 7 shows the center displacements versus time of a piezoceramic delaminated composite spherical shell with and without active control. It is observed that the displacements dampen with increase of control gain. It is also seen that the displacement damping becomes faster with higher control gain.

3.2 Effect of sensor/actuator patches

The effect of for sensor/actuator patch locations A1, B1, C1 and D1 on the transient response of delaminated composite spherical shell is investigated in Fig. 8. It is observed that the damping characteristic of the delaminated composite spherical shell itself depends on the location of patches. When the sensor/actuator pairs are closer the center (position D1) of the shell, the vibration control effect is best.

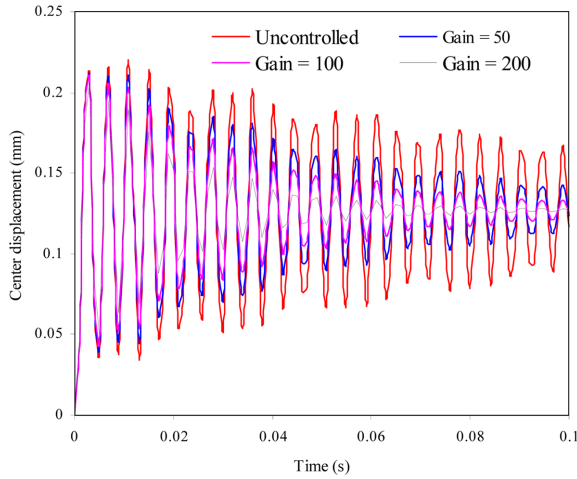


Fig. 7 Transient response of a piezoceramic delaminated composite spherical shell with and without active control

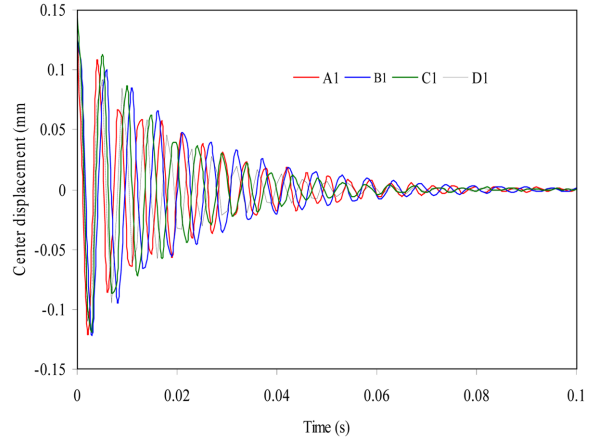


Fig. 8 Effect of sensor/actuator patch locations A1, B1, C1 and D1 on the transient response of delaminated composite spherical shell subjected to uniformly distributed load

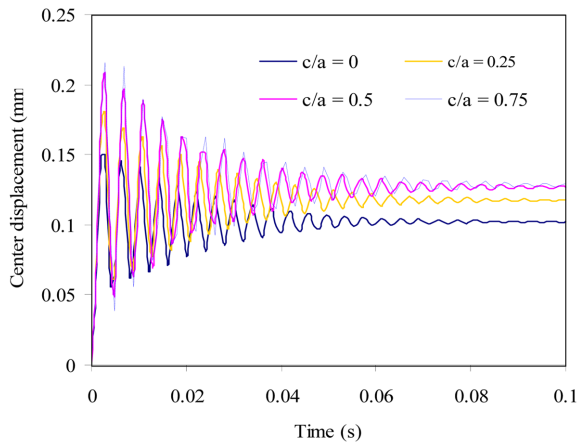


Fig. 9 Effect of delamination size on the transient response of piezoceramic composite spherical shell

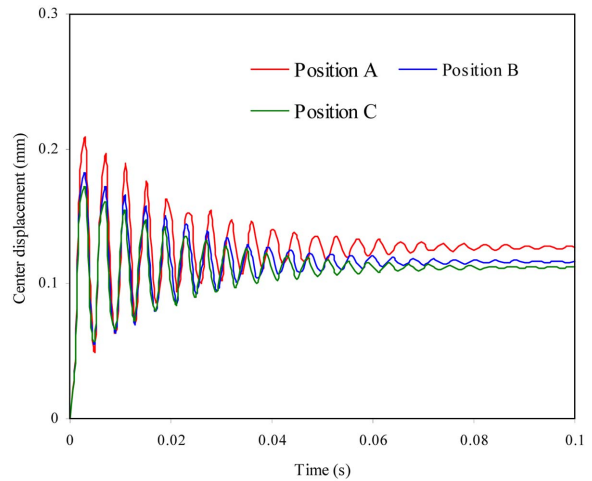


Fig. 10 Effect of delamination location on the transient response of piezoceramic composite spherical shell

3.3 Effect of delamination size

Next, the effect of delamination size on the transient response of piezoceramic composite spherical shell is studied and typical results are depicted in Fig. 9. For this, four different sizes of square mid-plane delamination having $c/a = 0$ (no delamination), 0.25, 0.5 and 0.75, and located at the center are considered. It is observed from the figure that the amplitude of center displacements increase with the increase of delamination size due to reduction in elastic stiffness of the shell. It is also observed that the delamination in the shell has reduced the damping characteristics when

compared to shell without delamination. The maximum displacement damping occurs for shell without delamination ($c/a = 0$).

3.4 Effect of delamination location

The effect of delamination location at the mid-plane on the transient response of piezoceramic composite spherical shell is presented in Fig. 10. It is observed from the figure that the amplitudes of center displacements decrease when the delamination is made eccentric (in y -direction, i.e. position B and both direction, i.e. position C) as compared to concentric delamination position (i.e. position A) thus making the shell stiffer. It can also be seen that the shells with eccentric position of delamination show a relatively improved damping performance compared to the centrally delaminated case.

3.5 Effect of radius of curvature to width ratio

Fig. 11 shows the effect of radius of curvature to width ratio (R/b) on the transient response of piezoceramic delaminated composite spherical shell. It is observed that the amplitude of center displacements increase with the increase of radius to width ratio (R/b) indicating that the stiffness is decreasing with the increase of R/b . Thus the shell with the smallest R/b shows the maximum displacement damping. However, the effect becomes minimal when $R/b \geq 100$. It is further seen that the displacement attains steady state with faster rate for higher R/b ratio.

3.6 Effect of shell types

Fig. 12 presents the transient response of four different piezoceramic delaminated composite shells viz, cylindrical ($R_y/R_x = 0$), spherical ($R_y/R_x = 1$), elliptic ($R_y/R_x = 2$) and hyperbolic paraboloids ($R_y/R_x = -1$) It is observed that the spherical shell has the smallest displacement amplitude and maximum damping. Further, the displacement amplitudes consistently increase and the damping

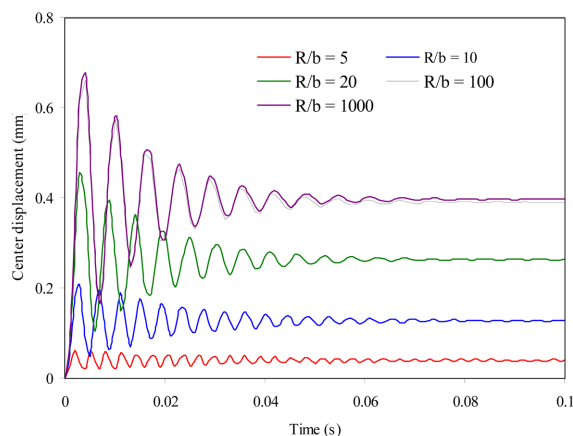


Fig. 11 Effect of radius to width ratio on the transient response of piezoceramic delaminated composite spherical shell

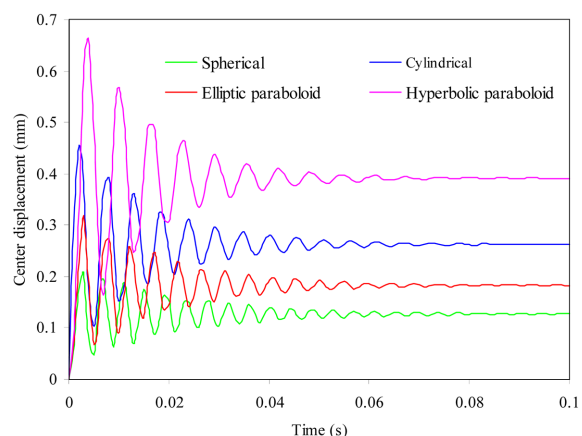


Fig. 12 Transient response of different piezoceramic delaminated composite shells

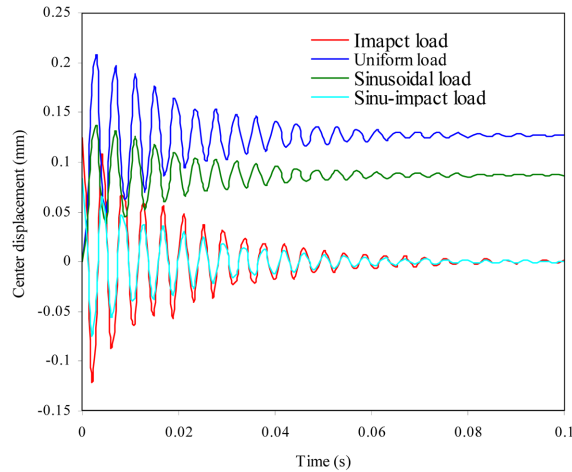


Fig. 13 Effect of loading conditions on the transient response of piezoceramic delaminated composite spherical shell

decrease for other shell forms in the order elliptic paraboloid, cylindrical and hyperbolic paraboloid. It is because of the fact that the spherical shell has the maximum average curvature $[(1/R_x)+(1/R_y)]/2$ followed by those of elliptic paraboloid, cylindrical shell and Hyperbolic paraboloid. It is to be noted that the hyperbolic paraboloid has zero average curvature.

3.7 Effect of loading conditions

The effect of applied loadings on the transient response of piezoceramic delaminated composite spherical shell is studied. Four different types of loading conditions, namely, uniformly distributed load, uniformly distributed impact load, sinusoidal load and sinusoidal impact loads are considered and results are depicted in Fig. 13. From the figure it is observed that the displacements under the uniformly distributed load and sinusoidal impact load have the highest and least responses, respectively.

4. Conclusions

The finite element method has been employed for the active control of dynamic response of delaminated composite shells with piezoelectric sensors and actuators. A simple negative feedback control algorithm coupling the direct and converse piezoelectric effects is used to actively control the dynamic response of delaminated composite shells in a closed loop. Time wise integration has been performed by Newmark's scheme. Efficacy of the present formulation is established. A good agreement among the available results is observed. The following conclusions are drawn from the detailed study:

- (1) The higher control gains significantly improve the damping characteristics of the delaminated composite shell as the center displacement dampens with increase of control gain.
- (2) The location of sensor/actuator patches affects the control performance of the structure. Here,

the best control effect is obtained when the patches are located at the center of a simply supported delaminated spherical shell.

(3) The displacement amplitude increase with the increase of delamination size for composite spherical shell. The delamination in shell has influenced both stiffening and damping effects.

(4) Displacement dampens out more effectively when the delamination position shifts from the center to the periphery in the mid-plane of the delaminated composite shells. Hence the location of delamination influences the damping performance of composite shells with piezoelectric patches.

(5) The displacement dampens out with faster rate for lower radius to width ratio possibly due to increase of stiffness. Thus, the geometric parameters influence the dynamic control of the delaminated composite shell.

(6) Relatively lower values of the center displacements of the spherical shell confirm its superiority to other doubly curved and cylindrical shells.

(7) The center displacement of the delaminated composite shell under uniformly distributed load is the maximum as compared to uniformly distributed impact load, sinusoidal load and sinusoidal impact loads.

It is worth mentioning that the present work opens a rich field of research on delaminated composite shells with piezoelectric sensor/actuators. There are enough scopes in applying other theories and methodologies to confirm and/or add new results in the field of active control of dynamic response of composite shells including debonding or delamination also.

Acknowledgements

The first author gratefully acknowledges the financial support provided by the CSIR (Council of Scientific and Industrial Research), New Delhi, India.

References

- Aymerich, F., Dore, F. and Priolo, P. (2009), "Simulation of multiple delaminations in impacted cross ply laminates using a finite element model based on cohesive interface elements", *Compos. Sci. Tech.*, **69**, 1699-1709.
- Balamurugan, V. and Narayanan, S. (2001), "Shell finite element for smart piezoelectric composite plate/shell structures and its applications to the study of active vibration control", *Finite Elem. Anal. D.*, **37**, 713-738.
- Bathe, K.J. (2001), *Finite Element Procedures*, Prentice-Hall of India Private Limited, New Delhi.
- Chandrashekhara, K. and Agarwal, A.N. (1993), "Active vibration control of laminated composite plates using piezoelectric devices: A finite element approach", *J. Int. Mat. Syst. Struct.*, **4**, 496-508.
- Chattopadhyay, A., Kim, H.S. and Ghoshal, A. (2004), "Nonlinear vibration analysis of smart composite structures with discrete delamination using a refined layerwise theory", *J. Sound Vib.*, **273**, 387-407.
- Ghoshal, A., Kim, H.S., Chattopadhyay, A. and Prosser, W.H. (2005), "Effect of delamination on transient history of smart composite plates", *Finite Elem. Anal. D.*, **41**, 850-874.
- Gim, C.K. (1994), "Plate finite element modeling of laminated plates", *Comput. Struct.*, **52**, 157-168.
- Hwang, W.S. and Park, H.C. (1993), "Finite element modeling of piezoelectric sensors and actuators", *AIAA J.*, **31**, 930-937.
- Ju, F., Lee, H.P. and Lee, K.H. (1995), "Finite element analysis of free vibration of delaminated composite plates", *Compos. Eng.*, **5**, 195-209.
- Kim, H.S., Chattopadhyay, A. and Ghoshal, A. (2003), "Characterization of delamination effect on composite laminates using a new generalized layerwise approach", *Comput. Struct.*, **81**, 1555-1566.
- Kim, H.S., Ghoshal, A., Kim, J. and Choi, S.B. (2006), "Transient analysis of delaminated smart composite structures by incorporating the Fermi-Dirac distribution function", *Smart Mater. Struct.*, **15**, 221-231.

- Kim, J.S. and Cho, M. (2003), "Efficient higher order shell theory for laminated composites with multiple delaminations", *AIAA J.*, **41**, 941-950.
- Kumar, R., Mishra, B.K. and Jain, S.C. (2008), "Static and dynamic analysis of smart cylindrical shell", *Finite Elem. Anal. D.*, **45**, 13-24.
- Lam, K.Y., Peng, X.Q., Liu, G.R. and Reddy, J.N. (1997), "A finite element model for piezoelectric composite laminates", *Smart Mater. Struct.*, **6**, 583-591.
- Lammering, R. (1991), "The application of a finite shell element for composite containing piezoelectric polymers in vibration control", *Comput. Struct.*, **41**, 1101-1109.
- Moita, J.M.S., Correia, I.F.P., Mota Soares, C.M. and Mota Soares, C.A. (2004), "Active control of adaptive laminated structures with bonded piezoelectric sensors and actuators", *Comput. Struct.*, **82**, 1349-1358.
- Oh, J., Cho, M. and Kim, J.S. (2005), "Dynamic analysis of composite plate with multiple delaminations based on higher order zigzag theory", *Int. J. Solid Struct.*, **42**, 6122-6140.
- Parhi, P.K., Bhattacharyya, S.S. and Sinha, P.K. (2001), "Hygrothermal effects on the dynamic behavior of multiple delaminated composite plates and shells", *J. Sound Vib.*, **248**, 195-214.
- Park, T. and Lee, S.Y. (2009), "Parametric instability of delaminated composite spherical shells subjected to in-plane pulsating forces", *Compos. Struct.*, **91**, 196-204.
- Park, T., Lee, S.Y. and Voyiadjis, G.Z. (2009), "Finite element vibration analysis of composite skew laminates containing delaminations around quadrilateral cutouts", *Composites: Part B*, **40**, 225-236.
- Ray, M.C. and Reddy, J.N. (2005), "Active control of laminated cylindrical shells using piezoelectric fiber reinforced composites", *Compos. Sci. Tech.*, **65**, 1226-1236.
- Reddy, J.N. (2004), *Mechanics of Laminated Composite Plates and Shells: Theory and Analysis*, CRC Press, Second Edition, Boca Raton, Florida.
- Samanta, B., Ray, M.C. and Bhattacharyya, R. (1996), "Finite element model for active control of intelligent structures", *AIAA J.*, **34**, 1885-1893.
- Sanders, J.L. (1959), "An improved first approximation theory for thin shells", NASA TR R-24.
- Shen, M.H.H. and Grady J.E. (1992), "Free vibrations of delaminated beams", *AIAA J.*, **30**, 1361-1370.
- Tiersten, H.F. (1969), *Linear Piezoelectric Plate Vibrations*, Plenum Press, New York.
- Tzou, H.S. and Tseng, C.I. (1990), "Distributed piezoelectric sensor/actuator design for dynamic measurement/control of distributed parameter systems: A piezoelectric finite element approach", *J. Sound Vib.*, **138**, 17-34.
- Vel, S.S. and Baillargeon, B.P. (2005), "Analysis of static deformation, vibration and active damping of cylindrical composite shells with piezoelectric shear actuators", *J. Vib. Acoust.*, **127**, 395-407.
- Wang, S.Y., Quek, S.T. and Ang, K.K. (2001), "Vibration control of smart piezoelectric composite plates", *Smart Mater. Struct.*, **10**, 637-644.
- Zhu, J.F., Gu, Y. and Tong, L. (2005), "Formulation of reference surface element and its applications in dynamic analysis of delaminated composite beams", *Compos. Struct.*, **68**, 481-490.